



## OPEN ACCESS

## EDITED BY

Xiaochu Zhang,  
University of Science and Technology of  
China, China

## REVIEWED BY

Yiheng Tu,  
Chinese Academy of Sciences (CAS), China  
Shaomin Zhang,  
Zhejiang University, China

## \*CORRESPONDENCE

Xiaoli Li

✉ xiaoli@bnu.edu.cn

RECEIVED 29 March 2024

ACCEPTED 22 April 2024

PUBLISHED 15 May 2024

## CITATION

Kang J, Li Y, Lv S, Hao P and Li X (2024)  
Effects of transcranial direct current  
stimulation on brain activity and cortical  
functional connectivity in children  
with autism spectrum disorders.  
*Front. Psychiatry* 15:1407267.  
doi: 10.3389/fpsy.2024.1407267

## COPYRIGHT

© 2024 Kang, Li, Lv, Hao and Li. This is an  
open-access article distributed under the terms  
of the [Creative Commons Attribution License  
\(CC BY\)](https://creativecommons.org/licenses/by/4.0/). The use, distribution or reproduction  
in other forums is permitted, provided the  
original author(s) and the copyright owner(s)  
are credited and that the original publication  
in this journal is cited, in accordance with  
accepted academic practice. No use,  
distribution or reproduction is permitted  
which does not comply with these terms.

# Effects of transcranial direct current stimulation on brain activity and cortical functional connectivity in children with autism spectrum disorders

Jiannan Kang<sup>1</sup>, Yuqi Li<sup>1</sup>, Shuaikang Lv<sup>1</sup>, Pengfei Hao<sup>1</sup>  
and Xiaoli Li<sup>2\*</sup>

<sup>1</sup>College of Electronic & Information Engineering, Hebei University, Baoding, China, <sup>2</sup>State Key Laboratory of Cognitive Neuroscience and Learning, Beijing Normal University, Beijing, China

**Introduction:** Transcranial direct current stimulation (tDCS) has emerged as a therapeutic option to mitigate symptoms in individuals with autism spectrum disorder (ASD). Our study investigated the effects of a two-week regimen of tDCS targeting the left dorsolateral prefrontal cortex (DLPFC) in children with ASD, examining changes in rhythmic brain activity and alterations in functional connectivity within key neural networks: the default mode network (DMN), sensorimotor network (SMN), and dorsal attention network (DAN).

**Methods:** We enrolled twenty-six children with ASD and assigned them randomly to either an active stimulation group (n=13) or a sham stimulation group (n=13). The active group received tDCS at an intensity of 1mA to the left DLPFC for a combined duration of 10 days. Differences in electrical brain activity were pinpointed using standardized low-resolution brain electromagnetic tomography (sLORETA), while functional connectivity was assessed via lagged phase synchronization.

**Results:** Compared to the typically developing children, children with ASD exhibited lower current source density across all frequency bands. Post-treatment, the active stimulation group demonstrated a significant increase in both current source density and resting state network connectivity. Such changes were not observed in the sham stimulation group.

**Conclusion:** tDCS targeting the DLPFC may bolster brain functional connectivity in patients with ASD, offering a substantive groundwork for potential clinical applications.

## KEYWORDS

autism spectrum disorder, electroencephalogram, transcranial direct current stimulation, sLORETA, lagged phase synchronization

## 1 Introduction

Autism Spectrum Disorder (ASD) encompasses a diverse range of neurodevelopmental conditions characterized by challenges in social communication, along with the presence of stereotyped, repetitive behaviors, and restricted interests. These symptoms, stemming from atypical nervous system development, emerged in early childhood, yet the pathogenesis remained elusive (1). Currently, interventions for children with ASD primarily consist of conventional rehabilitation therapies aimed at altering psychological states and rectifying abnormal behaviors through psychological and behavioral means to facilitate treatment outcomes. Nonetheless, targeted therapies for ASD are still under active investigation.

The emergence of non-invasive stimulation techniques in autism research has propelled transcranial direct current stimulation (tDCS) to the forefront. tDCS delivers a steady stream of electrical current to the cerebral cortex, modulating cortical excitability—it is both safe and non-invasive (2). tDCS influences neuronal excitability and plasticity by administering electrical currents and offers benefits such as mild stimulation intensity, affordability, and a reduced risk of adverse effects. Its application spans cognitive impairment, depression, and Alzheimer's disease treatments and rehabilitation research (3, 4) and showed promise for addressing cognitive deficits associated with neurological conditions (5). Importantly, tDCS does not require prolonged stillness from children, making it particularly suitable for children with ASD who may exhibit low functioning and hyperactivity. The modality also includes sham stimulation settings, accommodating the demands of clinical research. Cumulative evidence suggests that applying tDCS to the frontal cortex can markedly influence brain activities, including attention (6), learning (6–8), memory (7–9), and vigilance (10). These profound effects position tDCS as a potential therapeutic modality for ASD, although the efficacy of tDCS in children with ASD requires further exploration.

Resting-state Electroencephalogram (EEG) can reveal intrinsically connected functional networks, unobscured by the demands of cognitive tasks. While connectivity studies in EEG have traditionally relied on measurements between electrode pairs, this approach potentially suffers from volume conduction issues (11) and imprecise anatomical location estimates, assuming a two-dimensional construct rather than a true three-dimensional framework. Conversely, three-dimensional analysis utilizing EEG may furnish more intricate and accurate insights.

EEG source localization aims to identify sources of neural activity in the brain through potential differences between EEG electrodes on the scalp. An important development was the introduction of anatomical constraints on the head to facilitate the problem of EEG source location (12, 13). Further developments introduced physiological constraints of cortical sources to facilitate the solution of distributed source imaging (14). This prior constraint greatly improves the solvability and precision of brain source location. The distributed source model is based on thousands of orientationally fixed dipole sources that are regularly distributed in a three-dimensional (3D) brain space or cortical surface. The

activation of the source is described as a current density distribution. One advantage of the distributed model is that there is no need to make a prior assumption about the number of active dipoles under a particular scalp voltage diagram. The minimum norm algorithm was proposed in 1994 to estimate the source current distribution as an alternative to single or multiple dipole models. Since the minimum norm tends to mislocate deeper sources, the weighted minimum norm method can compensate for this with a weighted matrix. Low resolution electromagnetic Tomography (LORETA) aims to find the smoothest minimum norm solution to the EEG activity distribution, standardized LORETA (sLORETA) standardizes the current density estimate given by the minimum norm by using the covariance of the resolution matrix and is able to achieve zero error localization. We can examine EEG data through the lens of current source density measurements, made possible by standardized low-resolution electromagnetic tomography (sLORETA). This methodology synergized the high temporal resolution of EEG with the spatial localization of cerebral electrical activities (15). Correlation analysis revealed augmented short-range connectivity between regions implicated in the mirror neuron system and social perception networks (16). A previous magnetoencephalography investigation into ASD employed source localization to assess resting-state networks (RSN), including the default mode and salience networks (17). The findings associated reductions in gamma-band connectivity within the DMN and between the DMN and salience networks with ASD severity, particularly concerning social communication and interaction capacities. Historical focus has been scant on the sensorimotor network (SMN), which underlies core ASD symptoms due to atypical sensorimotor and perceptual processes (18–24). Moreover, studies regarding the functional brain networks sustaining attentional faculties are rare. The dorsal attention network (DAN) orchestrates goal-driven top-down control processes (25) and deficits in the connectivity within this network may underpin the attentional challenges characteristic of ASD (26, 27).

Hence, based on the above evidence, we conducted a shame-controlled trial to investigate the efficacy of tDCS in children with ASD. This study hypothesized that (1) significant differences of current source density in delta, theta, alpha, and beta rhythm in the DMN, SMN, and DAN would be observed between children with ASD and typically developing (TD) children. (2) active tDCS stimulation would increase current source density in the above described resting state networks and rhythms in the brain of children with ASD. (3) active tDCS stimulation would enhance functional connectivity (lagged phase synchronization) of resting-state networks in the brain of children with ASD.

## 2 Materials and methods

### 2.1 Subject information

Our study cohort consisted of 13 subjects (11 males and 2 females; mean age  $\pm$  SD:  $5.6 \pm 1.8$  years) undergoing 10 sessions of

tDCS treatment and a matched control group of 13 subjects (11 males and 2 females; mean age  $\pm$  SD:  $5.4 \pm 2.2$  years). All subjects were diagnosed with ASD by qualified psychiatrists according to the PEP-III (28) and DSM-IV-TR criteria (29). Informed consent was obtained in written form, with full comprehension of the experimental protocols provided to the parents beforehand. The clinical trial adhered to the Declaration of Helsinki and received approval from the Ethics Committee of the Affiliated Hospital of Hebei University.

Inclusion criteria for ASD subjects included (1) confirmation of autism by a certified child psychiatrist, (2) an age range of 4–6 years, and (3) provision of written informed consent. Exclusion criteria encompassed (1) a history of neurological diseases such as epilepsy, brain injury, or neurosurgery; (2) concurrent or prior use of antipsychotic or antiepileptic medications; and (3) previous exposure to tDCS, repetitive transcranial magnetic stimulation (rTMS), or neurofeedback interventions prior to this study.

## 2.2 EEG data acquisition

EEG recordings were conducted in an electromagnetically isolated environment, with subjects seated comfortably and wearing EEG caps, eyes open throughout the procedure. A parent and a trained expert were present to supervise the children and ensure the integrity of the data. Participants were gently encouraged to minimize blinking, with unmanageable eye movement artifacts subsequently removed during data preprocessing. Recordings lasted approximately 5–10 minutes and utilized a 128-channel HydroCel geodesic sensor net (Electrical Geodesics, Inc., Eugene, Oregon, USA), maintaining electrode impedance below 50 k $\Omega$ . Data was sampled at 1000 Hz using Cz as the reference electrode.

## 2.3 Data preprocessing

Data processing was performed off-line with Matlab R2016a and EEGLab V13.5.4b. Post-downsampling to 200 Hz, a 1–45 Hz band-pass filter was employed. Independent component analysis (ICA) (30) was used to remove artifacts linked to eye blinks, muscular movements, and electromyography. Data were then re-referenced to an average reference, and 19 electrodes were selected for further analysis according to the 10–20 system. EEG recordings for each participant were segmented into 24-second epochs, which were further divided into 3-second segments (8 per subject), and were systematically arranged within respective participant folders.

## 2.4 Stimulation procedure

Stimulation was performed using a 1 mA direct current delivered via a battery-powered stimulator (JX-tDCS-1, Huahengjingxing New Medical Technology Co., Ltd., Nanchang, China), with a consistent impedance below 10 k $\Omega$  between saline-soaked sponge electrodes ( $7 \times 4.5$  cm). For both active and sham

stimulation protocols, the anode was positioned on the left DLPFC, while the cathode was placed on the right supraorbital area. In the active tDCS condition, the current was gradually raised to 1 mA over 30 seconds, maintained for 20 minutes, and then decreased to zero within 30 seconds. The sham tDCS mirrored the electrode placement of the active stimulation but involved current flow merely for the initial 20 seconds.

## 2.5 Source location analysis and statistical nonparametric mapping

We utilized the sLORETA/eLORETA software package to estimate current source densities across 6239 cortical and hippocampal gray matter voxels, with a spatial resolution of 5 mm (15, 31). The voxel-by-voxel sLORETA data in various frequency bands—delta, theta, alpha, and beta—underwent analysis to discern differences between the ASD and TD groups, as well as within the active and sham tDCS-treated cohorts. The Statistical Nonparametric Mapping (SnPM) technique employed 5000 randomized, voxel-specific paired t-tests to perform comparative assessments. Prior to statistical evaluation, sLORETA images were logarithmically transformed to address non-specific regional confounds (32). Corrections for multiple comparisons were applied to the pooled SnPM results (33, 34). T-thresholds corresponding to a significance level of  $p < 0.05$  were calculated using statistical utilities from sLORETA.

## 2.6 Functional connectivity analysis

### 2.6.1 Region of interest

We derived ROIs for the SMN, DMN, and DAN following the framework established by Wantzen et al. (35), totaling 21 key areas. Each ROI encapsulated all gray matter voxels within a 10 mm radius, averaging the logarithmically transformed current densities across the voxels assigned to each ROI. Detailed names and corresponding coordinates of all regions are presented in Table 1.

### 2.6.2 Functional connectivity

Our study employed sLORETA to compute lagged phase synchronization for the functional connectivity analysis. This approach assesses signal similarity in the frequency domain, accounting for volume conduction and other non-physiological influences, thus providing a corrected phase synchronization value based on a normalized Fourier transform (22, 36). We assessed connectivity within networks by comparing lagged phase synchronization among ROIs for artifact-free EEG segments across the delta, theta, alpha, and beta bands. The log-transformed data underwent analysis using one-tailed t-statistics, with corrections for multiple comparisons achieved through a non-parametric permutation method involving 5000 randomizations. The derived t-thresholds reflect the designated significance level ( $p < 0.05$ ) for functional connectivity within the SMN, DAN, and DMN networks.

TABLE 1 Regions of interest.

|     | Regions                                  | MNI coordinates |
|-----|--|-----------------|
| DMN | Right Superior temporal gyrus            | 41 -60 29       |
|     | Left Superior temporal gyrus             | -41 -60 29      |
|     | Medial frontal gyrus                     | 0 49 18         |
|     | Posterior cingulate cortex               | 0 -52 26        |
| SMN | Right Precentral gyrus                   | 34 -32 59       |
|     | Left Postcentral gyrus                   | -44 -30 58      |
|     | Medial frontal gyrus                     | -4 -33 66       |
|     | Left Transverse temporal gyrus           | -56 -23 12      |
|     | Right Transverse temporal gyrus          | 55 -23 12       |
| DAN | Right Middle frontal gyrus               | 22 -8 54        |
|     | Left Middle frontal gyrus                | -22 -8 54       |
|     | Right Inferior parietal lobule           | 34 -38 44       |
|     | Left Inferior parietal lobule            | -34 -38 44      |
|     | Right Precuneus                          | 18 -69 51       |
|     | Left Precuneus                           | -18 -69 51      |
|     | Right Middle temporal gyrus              | 51 -64 -2       |
|     | Left Middle temporal gyrus               | -51 -64 -2      |
|     | Right Precuneus-superior parietal lobule | 8 -63 57        |
|     | Left Superior parietal lobule            | -8 -63 57       |
|     | Right Inferior frontal gyrus             | 49 3 34         |
|     | Left Inferior frontal gyrus              | -49 3 34        |

## 3 Results

### 3.1 Source location results

#### 3.1.1 Comparison of current source density between ASD group and TD group

Compared with the TD group, the source localization results across the delta, theta, alpha, and beta bands in the ASD group indicated that the current source density was significantly reduced.

Among them, the number of voxels with significant differences in delta band is 5418, the number of voxels with significant differences in theta band is 3603, the number of voxels with significant differences in alpha band is 3854, the number of voxels with significant differences in beta band is 5425. Specifically, delta band analysis revealed a notable decrease in the prefrontal and occipital regions, peaking in the middle occipital gyrus with a maximum value of ( $t_{max} = -7.319$ , xyz = 45, -85, 10) as depicted in Figure 1. Theta band observations showed substantial reduction in the occipital lobe, with the most significant value ( $t_{max} = -6.367$ , xyz = 50, -80, 10) situated in the middle temporal gyrus, illustrated in Figure 2. In the alpha band, reductions in current source density were eminent in the left frontal lobe, occipital lobe, and right temporal lobe, with the middle temporal gyrus showing the greatest difference ( $t_{max} = -6.550$ , xyz = 50, -80, 10), shown in Figure 3. Beta band results exhibited considerable decreases across the frontal, occipital, right temporal, and parietal lobes, with the middle frontal gyrus reflecting the highest discrepancy ( $t_{max} = -6.978$ , xyz = -5, 65, -15), demonstrated in Figure 4.

#### 3.1.2 Comparison of current source density before and after tDCS stimulation

In the active stimulation group, post-treatment source localization in the delta, theta, alpha, and beta bands indicated meaningful increases in current source density. Among them, the number of voxels with significant differences in delta band is 5910, the number of voxels with significant differences in theta band is 6039, the number of voxels with significant differences in alpha band is 6129, the number of voxels with significant differences in beta band is 5940. The delta band exhibited pronounced enhancements primarily in the frontal lobe, left parietal temporal lobe, and right occipital lobe, with the superior frontal gyrus presenting the highest increase ( $t_{max} = 7.514$ , xyz = -20, 55, 35), as shown in Figure 5. Theta band measurements displayed significant advancements in the frontal, parietal, occipital, and left temporal lobes, centered again in the superior frontal gyrus ( $t_{max} = 7.723$ , xyz = -20, 55, 35), represented in Figure 6. Sizable improvements in the alpha band spanned the frontal lobe, central area, parietal lobe, occipital lobe, and temporal lobe domains, with the middle occipital gyrus manifesting the foremost elevation ( $t_{max} = 7.122$ , xyz = 45, -85, 5), shown in Figure 7. For the beta band, notable enhancements were located in the frontal, temporal and right occipital regions, with the peak increase recorded in the superior frontal gyrus ( $t_{max} = 8.214$ , xyz = -25, 55, 30), exhibited in Figure 8. The sham stimulation group did not demonstrate significant changes.

### 3.2 Functional connectivity within brain networks

The results showed that functional connectivity in the brains of children in the ASD group was significantly reduced in DAN compared to the TD group. It is embodied between Left Middle temporal gyrus and Right Inferior frontal gyrus ( $t = -3.530$ ,  $p <$

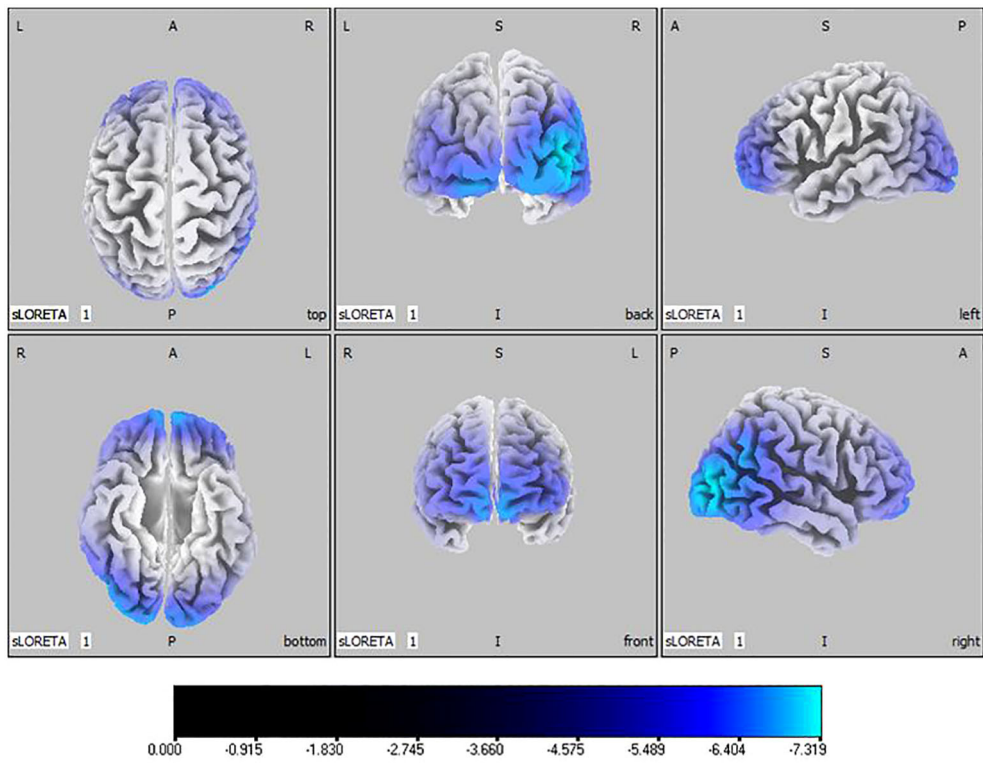


**FIGURE 1**  
 Source localization differences between ASD and TD groups in delta band: the blue areas denote significant reductions in current source density within the ASD group ( $p < 0.05$ ). Orientational abbreviations indicate the following: L for left hemisphere, R for right hemisphere, A for anterior (frontal) regions, P for posterior (rear) regions, and S for superior (upper) regions of the brain.

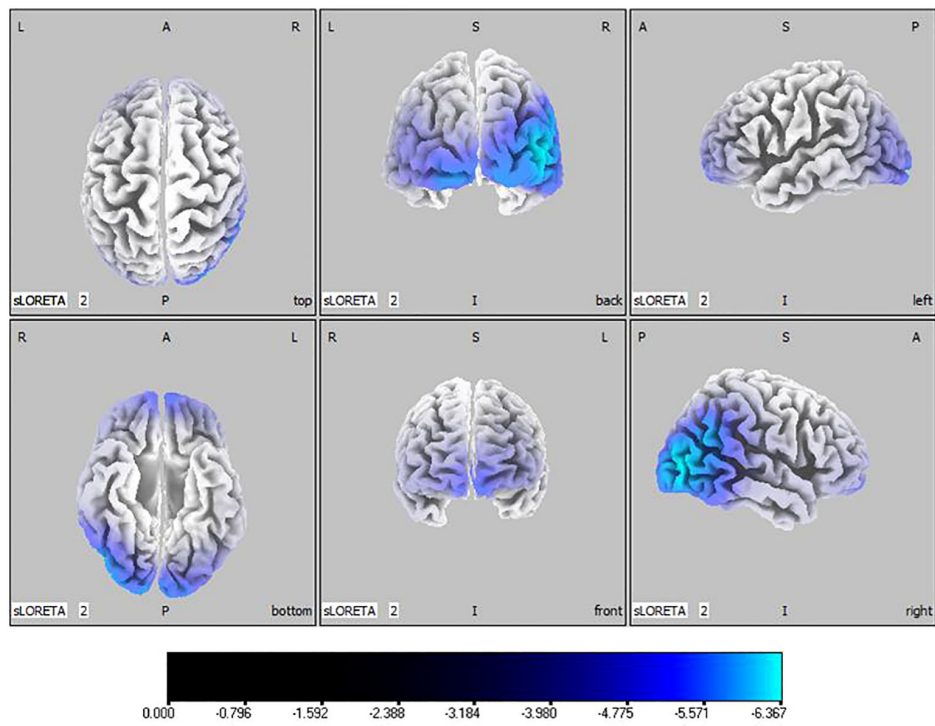


**FIGURE 2**  
 Source localization differences between ASD and TD groups in theta band: the blue areas denote significant reductions in current source density within the ASD group ( $p < 0.05$ ). Orientational abbreviations indicate the following: L for left hemisphere, R for right hemisphere, A for anterior (frontal) regions, P for posterior (rear) regions, and S for superior (upper) regions of the brain.

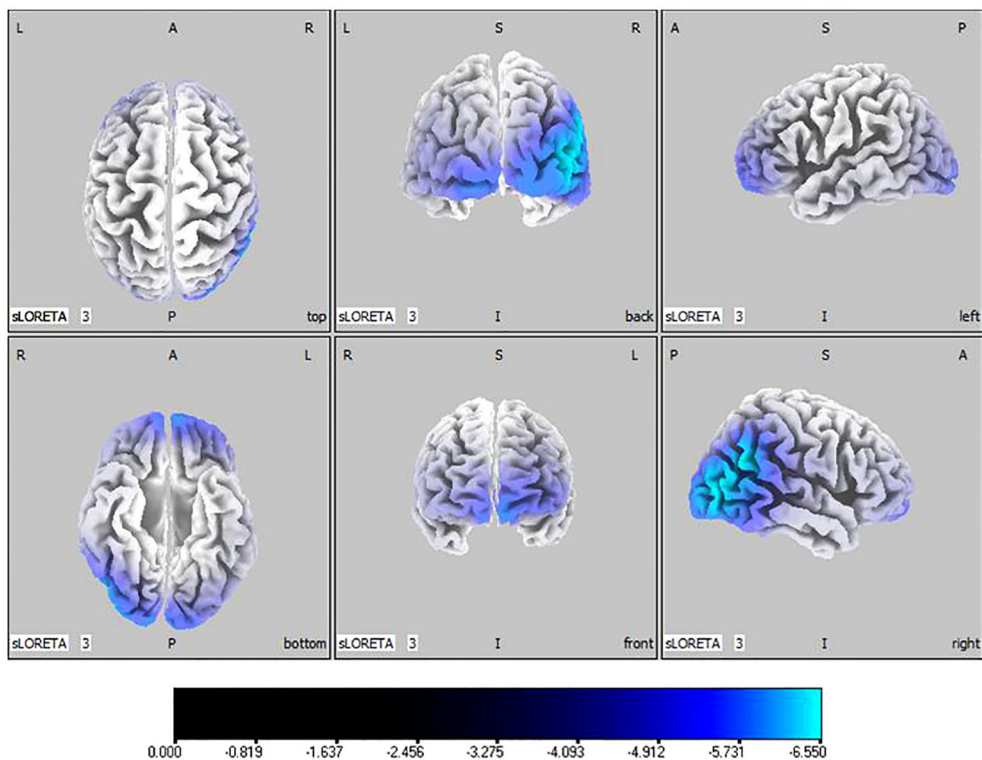


**FIGURE 3**  
 Source localization differences between ASD and TD groups in alpha band: the blue areas denote significant reductions in current source density within the ASD group ( $p < 0.05$ ). Orientational abbreviations indicate the following: L for left hemisphere, R for right hemisphere, A for anterior (frontal) regions, P for posterior (rear) regions, and S for superior (upper) regions of the brain.

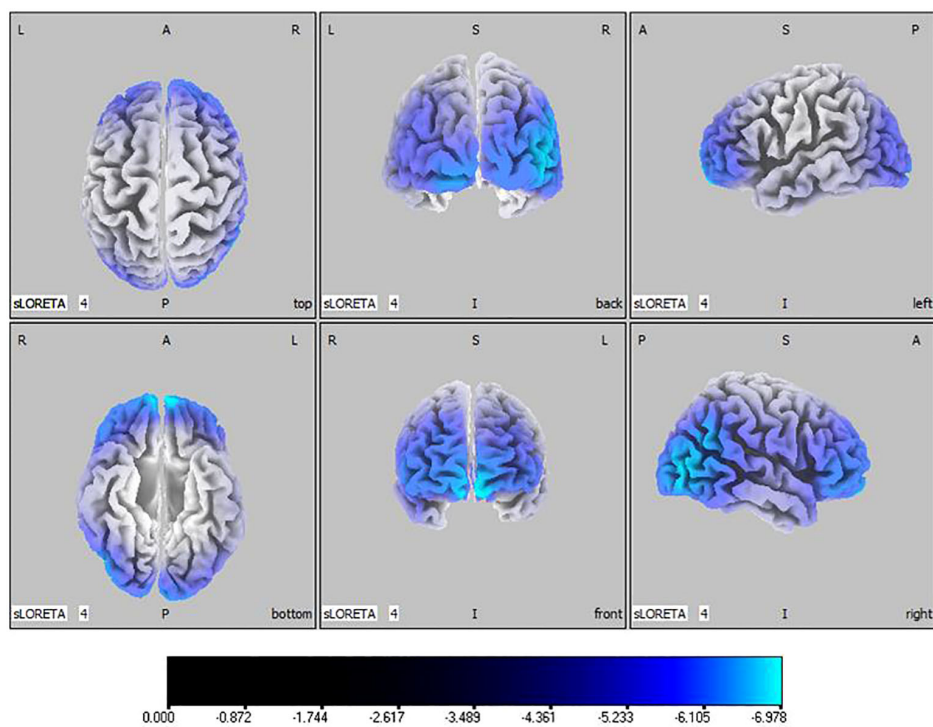


**FIGURE 4**  
 Source localization differences between ASD and TD groups in beta band: the blue areas denote significant reductions in current source density within the ASD group ( $p < 0.05$ ). Orientational abbreviations indicate the following: L for left hemisphere, R for right hemisphere, A for anterior (frontal) regions, P for posterior (rear) regions, and S for superior (upper) regions of the brain.

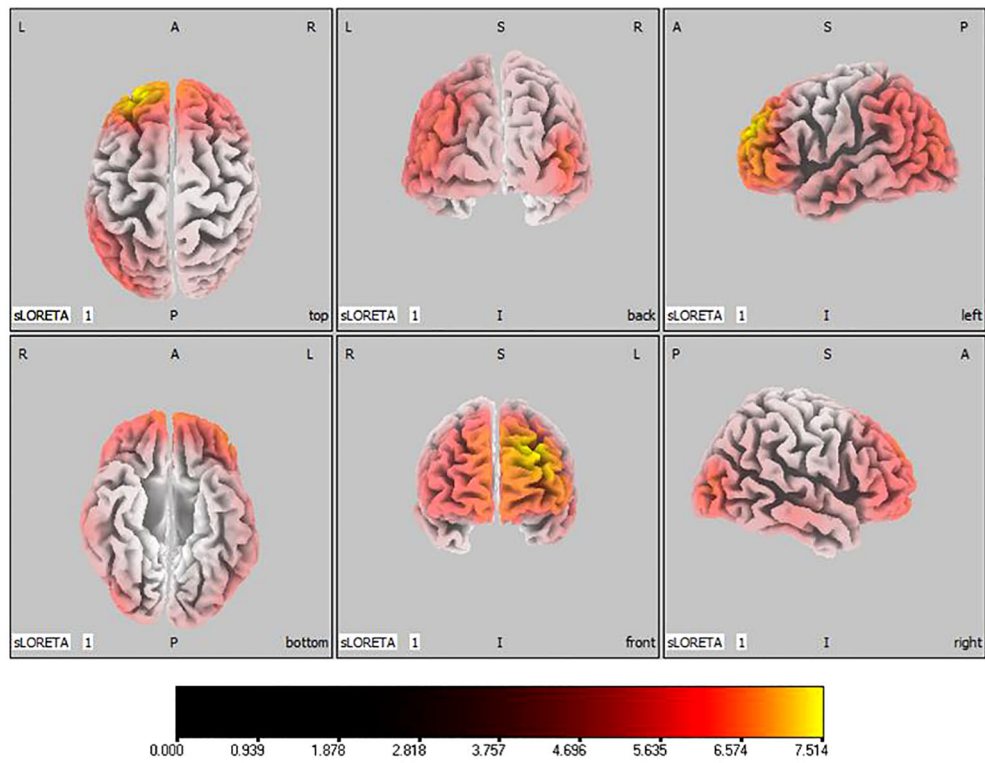


**FIGURE 5**  
 Source localization differences between pre-stimulation and post-stimulation groups in delta band. Red areas indicate the range in the post-stimulation group where the current source density increased significantly ( $p < 0.05$ ). Orientational abbreviations indicate the following: L for left hemisphere, R for right hemisphere, A for anterior (frontal) regions, P for posterior (rear) regions, and S for superior (upper) regions of the brain.

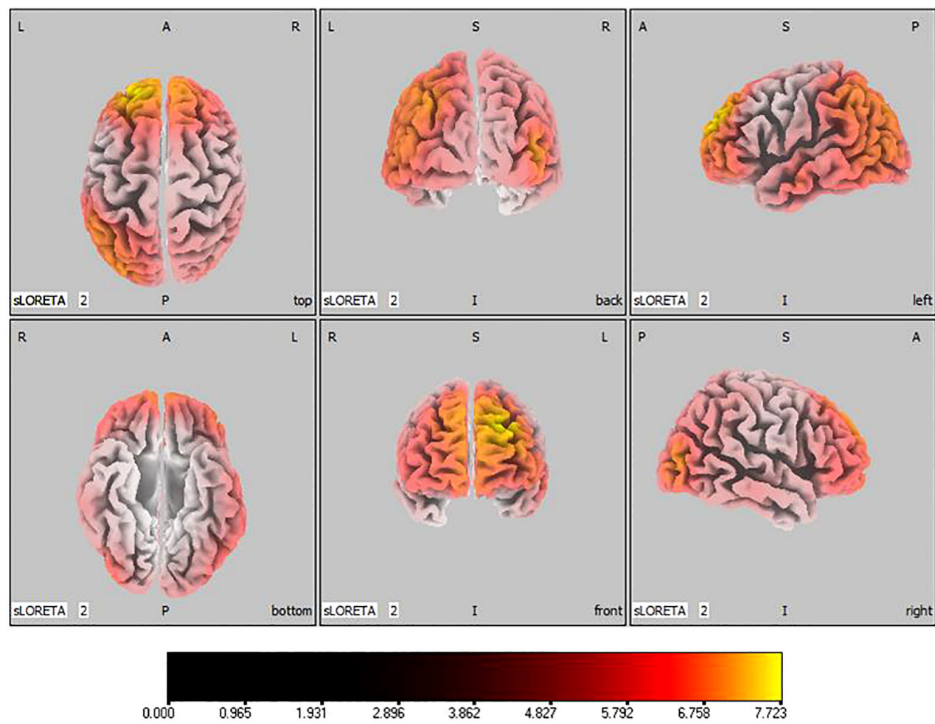


**FIGURE 6**  
 Source localization differences between pre-stimulation and post-stimulation groups in theta band. Red areas indicate the range in the post-stimulation group where the current source density increased significantly ( $p < 0.05$ ). Orientational abbreviations indicate the following: L for left hemisphere, R for right hemisphere, A for anterior (frontal) regions, P for posterior (rear) regions, and S for superior (upper) regions of the brain.

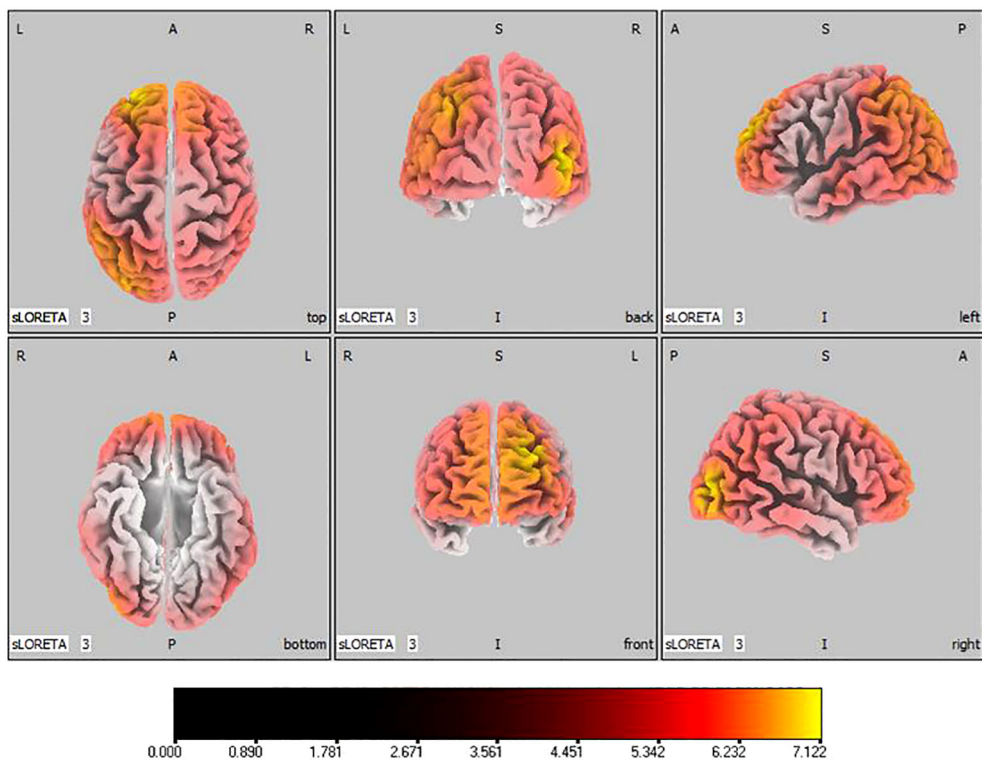


**FIGURE 7**  
 Source localization differences between pre-stimulation and post-stimulation groups in alpha band. Red areas indicate the range in the post-stimulation group where the current source density increased significantly ( $p < 0.05$ ). Orientational abbreviations indicate the following: L for left hemisphere, R for right hemisphere, A for anterior (frontal) regions, P for posterior (rear) regions, and S for superior (upper) regions of the brain.

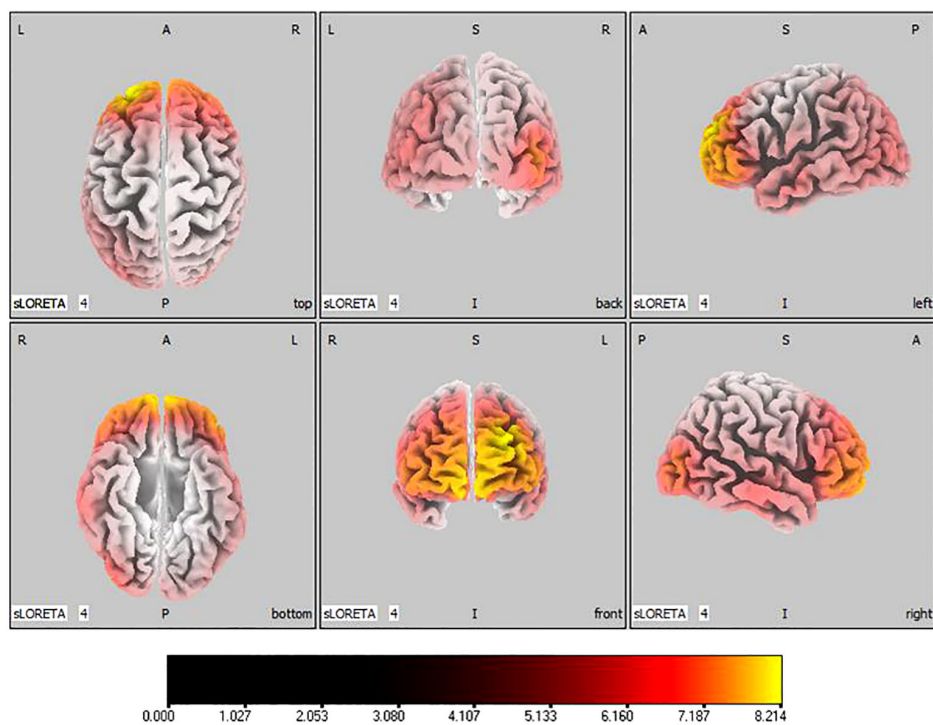


**FIGURE 8**  
 Source localization differences between pre-stimulation and post-stimulation groups in beta band. Red areas indicate the range in the post-stimulation group where the current source density increased significantly ( $p < 0.05$ ). Orientational abbreviations indicate the following: L for left hemisphere, R for right hemisphere, A for anterior (frontal) regions, P for posterior (rear) regions, and S for superior (upper) regions of the brain.

0.024) in theta band, as seen in Figure 9. There was no significant difference in functional connectivity between SMN and DMN.

In the active stimulation group, enhancements were observed in functional connectivity within brain networks post-intervention. The DMN displayed significant improvements particularly between the left superior temporal gyrus and medial frontal gyrus in the theta band ( $t = -2.431$ ,  $p < 0.048$ ), and between the right superior temporal gyrus and medial frontal gyrus in the beta band ( $t = -2.470$ ,  $p < 0.036$ ), as seen in Figure 10. Within the SMN, connectivity enhancements were primarily noted between the right precentral gyrus and right transverse temporal gyrus in the alpha band ( $t = -2.704$ ,  $p < 0.021$ ), and numerous regions in the beta band as elaborated in Figure 11. The DAN showed marked improvements, especially between the right middle temporal gyrus and right inferior frontal gyrus in the delta band ( $t = -2.626$ ,  $p < 0.021$ ), with additional connectivity augmentations displayed in various bands and areas as outlined in Figure 12. Contrarily, no statistically significant differences were reported in the sham stimulation cohort.

In examining the active stimulation group, our investigations illuminated significant findings within various neural networks of children with ASD, both preceding and following regulation. Our study's salient results are elucidated as follows:

### 3.2.1 Default mode network findings

In the DMN, we observed that ASD children exhibited significantly lower connectivity before regulation when compared to post-regulatory states. Notably, the connectivity rose notably between the left superior temporal gyrus and the medial frontal

gyrus within the theta frequency band ( $t = -2.431$ ,  $p < 0.048$ ). Furthermore, enhancements were apparent between the right superior temporal gyrus and the medial frontal gyrus in the beta frequency band ( $t = -2.470$ ,  $p < 0.036$ ), as depicted in Figure 10.

### 3.2.2 Sensorimotor network findings

Within the SMN, it was discerned that the brain connectivity in pre-regulation ASD children was significantly less than post-regulation. Such increments in connectivity manifested primarily between the right precentral gyrus and the right transverse temporal gyrus within the alpha frequency band ( $t = -2.704$ ,  $p < 0.021$ ). Additionally, rising connectivity was noted in the beta band between the left transverse temporal gyrus and various other brain regions—namely the right precentral gyrus ( $t = -3.657$ ,  $p < 0.001$ ), the left postcentral gyrus ( $t = -3.353$ ,  $p < 0.004$ ), the medial frontal gyrus ( $t = -3.858$ ,  $p < 0.006$ ), and the right transverse temporal gyrus ( $t = -2.785$ ,  $p < 0.021$ ). Moreover, between the right precentral gyrus and the medial frontal gyrus, a significant increase in connectivity was observed ( $t = -2.829$ ,  $p < 0.014$ ), presented in Figure 11.

### 3.2.3 Dorsal attention network findings

Contrasts within the DAN revealed that ASD children's pre-regulatory brain connectivity was substantially reduced compared to post-regulation. This was primarily seen between the right middle temporal gyrus and the right inferior frontal gyrus in the delta frequency band ( $t = -2.626$ ,  $p < 0.021$ ) and between the left inferior parietal lobe and the left inferior frontal gyrus in the theta band ( $t = -2.616$ ,  $p < 0.024$ ). In the alpha band, notable connectivity

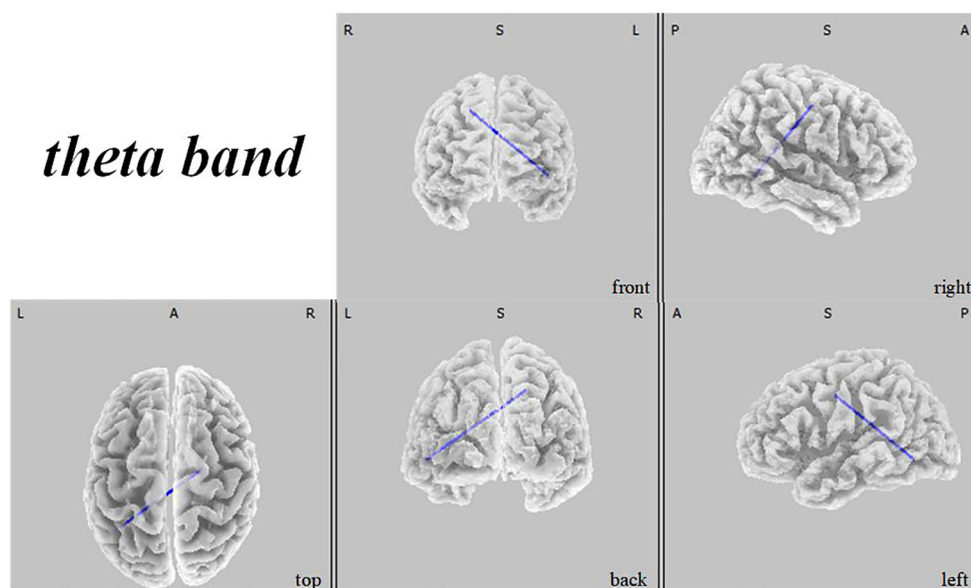


FIGURE 9

Connectivity variation diagram highlighting significant differences between ASD and TD groups. Blue lines represent a significant reduction in lagged phase synchronization within DAN for the pre-stimulation group as compared to the post-stimulation group. Orientation abbreviations indicate the following: L for left hemisphere, R for right hemisphere, A for anterior (frontal) regions, P for posterior (rear) regions, and S for superior (upper) regions of the brain.

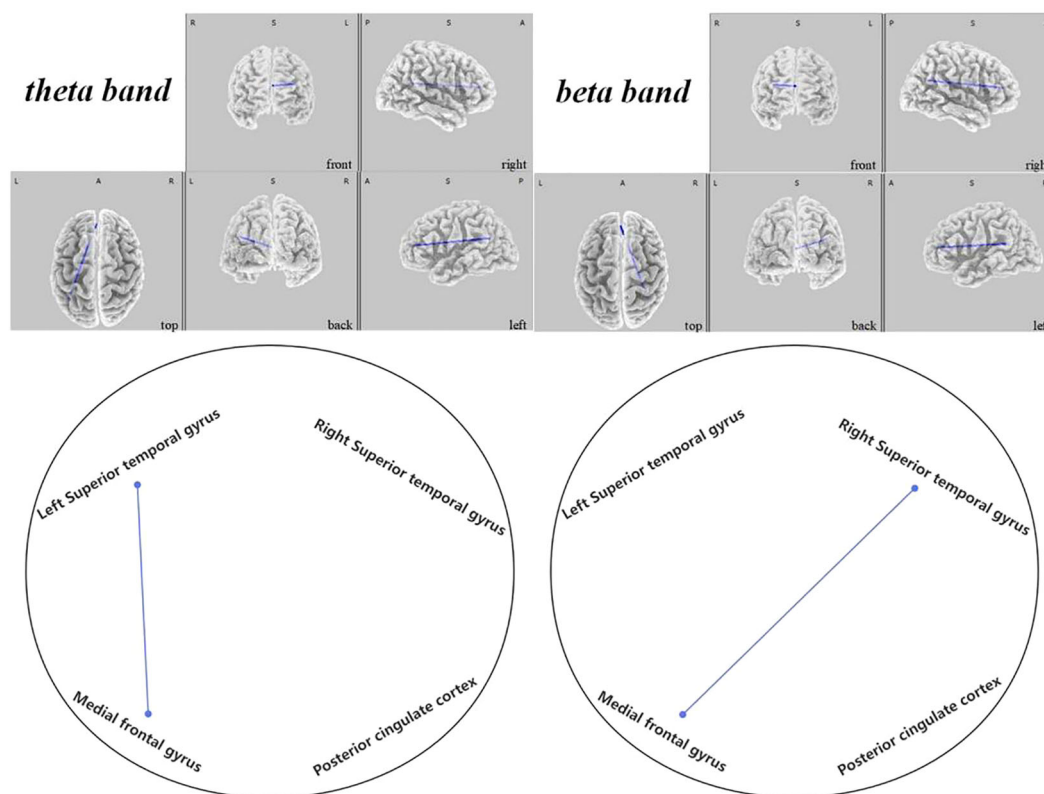


FIGURE 10

Connectivity variation diagram highlighting significant differences between pre-stimulation and post-stimulation groups. Blue lines represent a significant reduction in lagged phase synchronization within DMN for the pre-stimulation group as compared to the post-stimulation group. Orientational abbreviations indicate the following: L for left hemisphere, R for right hemisphere, A for anterior (frontal) regions, P for posterior (rear) regions, and S for superior (upper) regions of the brain.

enhancements could be observed (1) between the right inferior parietal lobule and the right middle frontal gyrus ( $t = -2.484$ ,  $p < 0.04$ ), the left inferior parietal lobule ( $t = -3.645$ ,  $p < 0.015$ ), and the right precuneus-superior parietal lobule ( $t = -3.143$ ,  $p < 0.005$ ), (2) as well as between the left middle temporal gyrus and the left inferior frontal gyrus ( $t = -3.239$ ,  $p < 0.001$ ). Similarly, beta band findings revealed significant connections (1) between the right middle frontal gyrus and the left middle temporal gyrus ( $t = -2.960$ ,  $p < 0.012$ ), (2) bridging between the left and right precuneus ( $t = -2.346$ ,  $p < 0.048$ ), (3) and from the left superior parietal lobule to the right middle frontal gyrus ( $t = -2.555$ ,  $p < 0.033$ ), the left precuneus ( $t = -2.683$ ,  $p < 0.018$ ), and the right precuneus ( $t = -2.538$ ,  $p < 0.039$ ), (4) further linking the left middle frontal gyrus with the right inferior parietal lobule ( $t = -3.171$ ,  $p < 0.006$ ).

## 4 Discussion

In this study, we evaluated the variations in current source density across the delta, theta, alpha, and beta bands within the brains of children diagnosed with ASD in comparison to typically developing children, as well as the changes in ASD children before and after

undergoing tDCS stimulation. Utilizing lagged phase synchronization via sLORETA, we've examined functional connectivity alterations within three brain resting states before and after tDCS. Our findings indicated a notably lower current source density in the neural architecture of children in the ASD group when compared to the TD group. Post-tDCS regulation, the active stimulation group exhibited a substantial enhancement in brain current source density, which wasn't observed in the sham stimulation group. Notably, ASD children's brain activation improved significantly following tDCS intervention, with an increased number and distribution of voxels showing significant differences.

There is a well-documented array of evidence suggesting that individuals with ASD possess atypical brain structures and functioning (37–39), and non-invasive brain stimulation methods such as tDCS have demonstrated a considerable impact on modulating both brain activity and connective function (40, 41). Active tDCS stimulation, in contrast with sham, has been shown to reduce resting-state functional connections (42). Correspondingly, our study recorded a noteworthy rise in lagged phase synchronization within the DMN, SMN, and DAN in children with ASD post tDCS stimulation.

Existing research indicates that anomalous intrinsic functional connectivity of brain networks is a central aspect of social

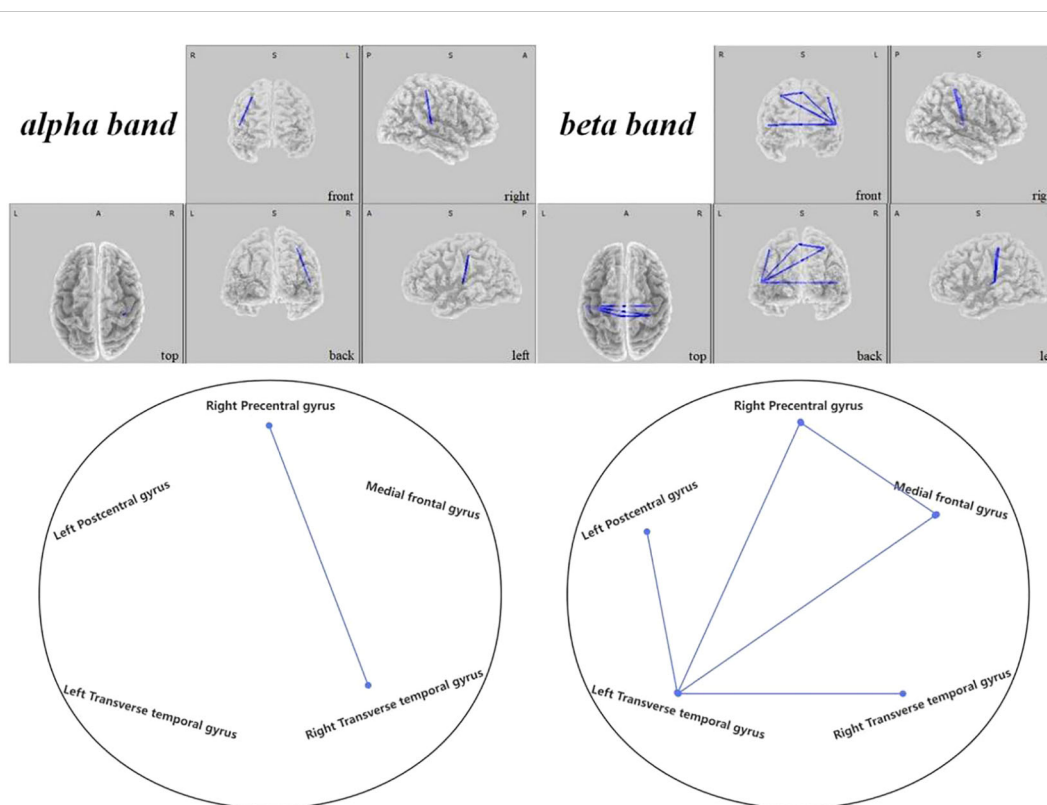


FIGURE 11

Connectivity variation diagram highlighting significant differences between pre-stimulation and post-stimulation groups. Blue lines represent a significant reduction in lagged phase synchronization within SMN for the pre-stimulation group as compared to the post-stimulation group. Orientational abbreviations indicate the following: L for left hemisphere, R for right hemisphere, A for anterior (frontal) regions, P for posterior (rear) regions, and S for superior (upper) regions of the brain.

impairments in ASD (43). Moreover, the DMN—which plays a crucial role in processing self and other-related information and is implicated in recollecting episodic and autobiographical memories (44), as well as understanding others' mental states (45)—has emerged as a pivotal system contributing to social deficits in ASD (46, 47). In line with this, our study discerned enhanced connectivity in the DMN between the medial frontal gyrus and bilateral superior temporal gyres in children with ASD post tDCS, which may significantly remodel internal information processing, potentially easing social impairments in ASD (48).

As a neural sensor, the SMN is primarily engaged in the handling and transmission of sensory and motor information. The interconnections between the different areas within this network ensure precise coordination of sensory and motor function. Diminished connectivity within the somatosensory and motor networks corroborates the atypical multisensorial and motor integration seen in ASD patients, likely contributing to core symptoms (49, 50). Our findings suggest that tDCS stimulation may elevate responsiveness to sensory input in individuals with ASD, thereby enhancing multisensory integration and consequently improving social capacities (51–53).

The DAN is recognized as a bilateral network that sustains attentional stability and contributes to the varying aspects of intelligence development (25, 54). Given the plethora of sensory

signals the brain continually receives; DAN enables prioritization of attention to the foremost inputs at any given moment (55). Aberrations in DAN functional connectivity can manifest as impaired attention and hindered top-down processing in ASD. Following stimulation, increased connectivity within key DAN regions in our study might bolster attentional control and top-down goal-directed processing in individuals with ASD (25).

Thus, our research demonstrates that tDCS stimulation is safe and reliable, and may amplify brain activity and augment functional connectivity in individuals with ASD, potentially ameliorating core symptoms. And our study shows that tDCS can be applied to clinical treatment for a long time, and has far-reaching significance to improve the status quo of autistic children. Nevertheless, the employment of tDCS as a therapeutic approach for ASD remains in its nascent stages, with our study facing certain limitations. Firstly, our research depended on a relatively modest sample size with broader samples required in future inquiries. Additionally, evaluations were only conducted at two points—baseline and post-treatment. Subsequent research should incorporate multiple assessments, including follow-ups, to capture critical trajectories of tDCS' effects. Thirdly, our study solely focused on the left DLPFC as a target area for tDCS, despite emerging studies that suggest various potential targets each potentially addressing specific ASD symptoms. Future

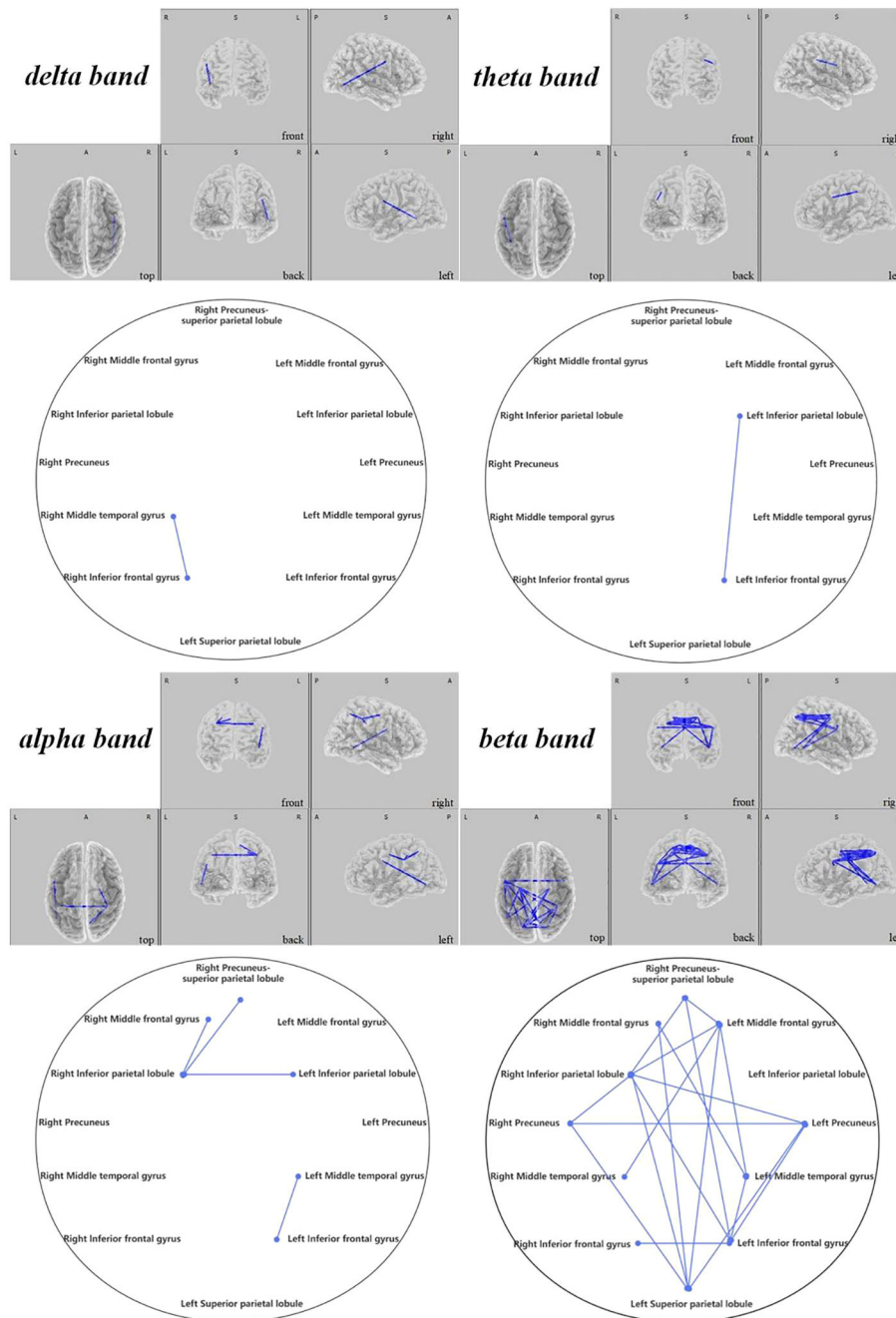


**FIGURE 12**  
 Connectivity variation diagram highlighting significant differences between pre-stimulation and post-stimulation groups. Blue lines represent a significant reduction in lagged phase synchronization within DAN for the pre-stimulation group as compared to the post-stimulation group. Orientational abbreviations indicate the following: L for left hemisphere, R for right hemisphere, A for anterior (frontal) regions, P for posterior (rear) regions, and S for superior (upper) regions of the brain.

investigations must explore these alternative sites. Lastly, while sLORETA serves as our means to measure brain activity and delineate regions, it is not without spatial limitations.

In conclusion, this study employed sLORETA to elucidate differences in brain activity between children with ASD and their TD counterparts, demonstrating that tDCS intervention in

the DLPFC can enhance brain connectivity and evidencing the positive neuromodulatory effects of tDCS. Conferring the possibility that tDCS may emerge as a promising therapeutic avenue for children with ASD, its clinical application could become increasingly widespread, adding valuable practicality in clinical settings.

## Data availability statement

The raw data supporting the conclusions of this article will be made available by the corresponding author on reasonable request.

## Ethics statement

The studies involving humans were approved by the Ethics Committee of the Affiliated Hospital of Hebei University. The studies were conducted in accordance with the local legislation and institutional requirements. Written informed consent for participation in this study was provided by the participants' legal guardians/next of kin.

## Author contributions

XL: Writing – review & editing, Funding acquisition, Conceptualization. JK: Writing – original draft, Supervision. YL: Writing – review & editing, Formal analysis, Data curation. SL: Writing – review & editing, Software, Investigation, Data curation. PH: Writing – review & editing, Supervision, Methodology.

## References

- Maenner MJ, Shaw KA, Baio J, Washington A, Dietz PM. Prevalence of autism spectrum disorder among children aged 8 years—autism and developmental disabilities monitoring network, 11 sites, United States, 2016. *MMWR Surveillance summaries: Morbid mortal week Rep Surveillance summaries / CDC.* (2020) 69:1–12. doi: 10.15585/mmwr.ss6706a
- Luckhardt C, Boxhoorn S, Schtz M, Fann N, Christine MF, et al. Brain stimulation by tDCS as treatment option in Autism Spectrum Disorder: a systematic literature review. *Prog Brain Res.* (2021) 264:233–57. doi: 10.1016/bs.pbr.2021.03.002
- Aksu S, Uslua I, Scen P, Barham H, Bilgic B, Hanagasi H, et al. Does transcranial direct current stimulation enhance cognitive performance in Parkinson's disease mild cognitive impairment? An event-related potentials and neuro psychological assessment study. *Neurol Sci.* (2022) 43:4029–44. doi: 10.1007/s10072-022-06020-z
- Rajji TK, Bowie CR, Herrmann N, Pollock BG, Bikson M, Blumberger DM, et al. Design and rationale of the PACt-MD randomized clinical trial: prevention of Alzheimer's dementia with cognitive remediation plus transcranial direct current stimulation in mild cognitive impairment and depression. *J Alzheimers Dis.* (2020) 76:733–51. doi: 10.3233/JAD-200141
- Sun X, Allison C, Wei L, Matthews FE, Wu Y, Auyeung B, et al. Autism prevalence in China is comparable to Western prevalence. *Mol Autism.* (2019) 10:7. doi: 10.1186/s13229-018-0246-0
- Clark VP, Parasuraman R. Neuroenhancement: enhancing brain and mind in health and in disease. *NeuroImage.* (2014) 85:889–94. doi: 10.1016/j.neuroimage.2013.08.071
- Coffman BA, Clark VP, Parasuraman R. Battery powered thought: enhancement of attention, learning, and memory in healthy adults using transcranial direct current stimulation. *NeuroImage.* (2014) 85:895–908. doi: 10.1016/j.neuroimage.2013.07.083
- Floel A. tDCS-enhanced motor and cognitive function in neurological diseases. *NeuroImage.* (2014) 85:934–47. doi: 10.1016/j.neuroimage.2013.05.098
- Ferrucci R, Priori A. Transcranial cerebellar direct current stimulation (tcDCS): motor control, cognition, learning and emotions. *NeuroImage.* (2014) 85:918–23. doi: 10.1016/j.neuroimage.2013.04.122
- Nelson JT, McKinley RA, Golob EJ, Warm JS, Parasuraman R. Enhancing vigilance in operators with prefrontal cortex transcranial directcurrent stimulation (tDCS). *NeuroImage.* (2014) 85:909–17. doi: 10.1016/j.neuroimage.2012.11.061
- Nunez PL, Silberstein RB, Cadusch PJ, Wijesinghe RS, Westdorp AF, Srinivasan R. A theoretical and experimental study of high resolution EEG based on surface Laplacians and cortical imaging. *ElectroencephalogrClin Neurophysiol.* (1994) 90:40–57. doi: 10.1016/0013-4694(94)90112-0

## Funding

The author(s) declare financial support was received for the research, authorship, and/or publication of this article. This research was funded in part by the National Natural Science Foundation of China (82151304) and all the subjects and their parents.

## Conflict of interest

The authors declare that the research was conducted in the absence of any commercial or financial relationships that could be construed as a potential conflict of interest.

## Publisher's note

All claims expressed in this article are solely those of the authors and do not necessarily represent those of their affiliated organizations, or those of the publisher, the editors and the reviewers. Any product that may be evaluated in this article, or claim that may be made by its manufacturer, is not guaranteed or endorsed by the publisher.

- He B, Musha T, Okamoto Y, Homma S, Nakajima Y, Sato T, et al. Electric dipole tracing in the brain by means of the boundary element method and its accuracy. *IEEE Trans BioMed Eng.* (1987) 34:406–14. doi: 10.1109/TBME.1987.326056
- Hämäläinen M, Sarvas J. Realistic conductor geometry model of the human head for interpretation of neuromagnetic data. *IEEE Trans BioMed Eng.* (1989) 36:165–71. doi: 10.1109/10.16463
- Dale AM, Sereno MI. Improved localization of cortical activity by combining EEG and MEG with MRI cortical surface reconstruction: a linear approach. *J Cognit Neurosci.* (1993) 5:162–76. doi: 10.1162/jocn.1993.5.2.162
- Pascual-Marqui RD. Standardized low-resolution brain electromagnetic tomography (sLORETA): technical details, Methods Find Exp. *Clin Pharmacol.* (2002) 24(Suppl D):5–12. doi: 10.1002/med.10000
- Coben R, Mohammad-Rezazadeh I, Cannon RL. Using quantitative and analytic EEG methods in the understanding of connectivity in autism spectrum disorders: a theory of mixed over- and under-connectivity. *Front Hum Neurosci.* (2014) 8. doi: 10.3389/fnhum.2014.00045
- Lajiness-O'Neill R, Brennan JR, Moran JE, Richard AE, Flores AM, Swick C, et al. Patterns of altered neural synchrony in the default mode network in autism spectrum disorder revealed with magnetoencephalography (MEG): relationship to clinical symptomatology. *Autism Res Off J Int Soc Autism Res.* (2018) 11:434–49. doi: 10.1002/aur.1908
- Perry W, Minassian A, Lopez B, Maron L, Lincoln A. Sensorimotor gating deficits in adults with autism. *Biol Psychiatry.* (2007) 61:482–6. doi: 10.1016/j.biopsych.2005.09.025
- Takarae Y, Minshew NJ, Luna B, Sweeney JA. Atypical involvement of frontostriatal systems during sensorimotor control in autism. *Psychiatry Res Neuroimag.* (2007) 156:117–27. doi: 10.1016/j.psychres.2007.03.008
- Travers BG, Kana RK, Klinger LG, Klein CL, Klinger MR. Motor learning in individuals with autism spectrum disorder: activation in superior parietal lobule related to learning and repetitive behaviors. *Autism Res Off J Int Soc Autism Res.* (2015) 8:38–51. doi: 10.1002/aur.1403
- Boyd BA, Baranek GT, Sideris J, Poe MD, Watson LR, Patten E, et al. Sensory features and repetitive behaviors in children with autism and developmental delays. *Autism Res Off J Int Soc Autism Res.* (2010) 3:78–87. doi: 10.1002/aur.124
- Cascio CJ, Woynaroski T, Baranek GT, Wallace MT. Toward an interdisciplinary approach to understanding sensory function in autism spectrum disorder. *Autism Res.* (2016) 9:920–5. doi: 10.1002/aur.1612

23. Foss-Feig JH, Heacock JL, Cascio CJ. Tactile responsiveness patterns and their association with core features in autism spectrum disorders. *Res Autism Spectr Disord.* (2012) 6:337–44. doi: 10.1016/j.rasd.2011.06.007
24. Lim YH, Partridge K, Girdler S, Morris SL. Standing postural control in individuals with autism spectrum disorder: systematic review and meta-analysis. *J Autism Dev Disord.* (2017) 47:2238–53. doi: 10.1007/s10803-017-3144-y
25. Corbetta M, Shulman GL. Control of goal-directed and stimulus-driven attention in the brain. *Nat Rev Neurosci.* (2002) 3:201–15. doi: 10.1038/nrn755
26. Xan B, Zhao J, Xu Q, Sun Q, Wang Z. Abnormal functional connectivity of resting state network detection based on linear ICA analysis in autism spectrum disorder. *Front Physiol.* (2018) 9. doi: 10.3389/fphys.2018.00475
27. Farrant K, Uddin LQ. Atypical developmental of dorsal and ventral attention networks in autism. *Dev Sci.* (2016) 19:550–63. doi: 10.1111/desc.12359
28. Chen KL, Chiang FM, Tseng MH, Fu CP, Hsieh CL. Responsiveness of the psychoeducational profile-third edition for children with autism spectrum disorders. *J Autism Dev Disord.* (2011) 41:1658–64. doi: 10.1007/s10803-011-1201-5
29. Sadler JZ, Fulford B. Normative warrant in diagnostic criteria: the case of DSM-IV-TR personality disorders. *J Pers Disord.* (2006) 20:170–80. doi: 10.1521/pedi.2006.20.2.170
30. Xie JW, Douglas PK, Wu YN, Brody AL, Anderson AE. Decoding the encoding of functional brain networks: An fMRI classification comparison of non-negative matrix factorization (NMF), independent component analysis (ICA), and sparse coding algorithms. *J Neurosci Methods.* (2017) 282:81–94. doi: 10.1016/j.jneumeth.2017.03.008
31. Pascual-Marqui RD, Lehmann D, Koukkou M, Kochi K, Anderer P, Saletu B, et al. Assessing interactions in the brain with exact low-resolution electromagnetic tomography. *Philos. Trans A Math Phys Eng Sci.* (2011) 369:3768–84. doi: 10.1098/rsta.2011.0081
32. Gianotti LRR, Dahinden FM, Baumgartner T, Knoch D. Understanding individual differences in domain-general prosociality: a resting EEG study. *Brain Topogr.* (2019) 32:118–26. doi: 10.1007/s10548-018-0679-y
33. Holmes AP, Blair RC, Watson JD, Ford I. Nonparametric analysis of statistic images from functional mapping experiments. *J Cereb Blood Flow Metab Off J Int Soc Cereb Blood Flow Metab.* (1996) 16:7–22. doi: 10.1097/00004647-199601000-00002
34. Nichols TE, Holmes AP. Nonparametric permutation tests for functional neuroimaging: a primer with examples. *Hum Brain Mapp.* (2002) 15:1–25. doi: 10.1002/hbm.1058
35. Wantzen P, Clochon P, Doidy F, Wallois F, Mahmoudzadeh M, Desauvay P, et al. EEG resting-state functional connectivity: evidence for an imbalance of external/internal information integration in autism. *J Neurodevel Disord.* (2022) 14:47. doi: 10.1186/s11689-022-09464-8
36. Pascual-Marqui RD, Lehmann D, Koukkou M, Kochi K, Anderer P, Saletu B, et al. Assessing interactions in the brain with exact low-resolution electromagnetic tomography. *Philos Transact A Math Phys Eng Sci.* (2011) 369:3768–84. doi: 10.1098/rsta.2011.0081
37. Cardinale RC, Shih P, Fishman I, Ford LM, Müller RA. Pervasive rightward asymmetry shifts of functional networks in autism spectrum disorder. *JAMA Psychiatry.* (2013) 70:975–82. doi: 10.1001/jamapsychiatry.2013.382
38. Pascual-Leone A, Freitas C, Oberman L, Horvath JC, Halko M, Eldaief M, et al. Characterizing brain cortical plasticity and network dynamics across the age-span in health and disease with TMS-EEG and TMS-fMRI. *Brain Topogr.* (2011) 24:302–15. doi: 10.1007/s10548-011-0196-8
39. Verhoeven JS, De Cock P, Lagae L, Sunaert S. Neuroimaging of autism. *Neuroradiology.* (2010) 52:3–14. doi: 10.1007/s00234-009-0583-y
40. Esmailpour Z, Shereen AD, Ghobadi-Azbari P, Datta A, Woods AJ, Ironside M, et al. Methodology for tDCS integration with fMRI. *Hum Brain Mapp.* (2020) 41:1950–67. doi: 10.1002/hbm.24908
41. Vosskuhl J, Struber D, Herrmann CS. Non-invasive brain stimulation: a paradigm shift in understanding brain oscillations. *Front Hum Neurosci.* (2018) 12:211. doi: 10.3389/fnhum.2018.00211
42. Antonenko D, Schubert F, Bohm F, Ittermann B, Aydin S, Hayek D, et al. tDCS-induced modulation of GABA levels and resting-state functional connectivity in older adults. *J Neurosci.* (2017) 37:4065–73. doi: 10.1523/JNEUROSCI.0079-17.2017
43. Müller RA, FISHMAN I. Brain connectivity and neuroimaging of social networks in autism. *Trends Cognit Sci.* (2018) 22:1103–16. doi: 10.1016/j.tics.2018.09.008
44. Spreng RN, Mar RA, Kim AS. The common neural basis of autobiographical memory, prospection, navigation, theory of mind, and the default mode: A quantitative meta-analysis. *J Cognit Neurosci.* (2009) 21:489–510. doi: 10.1162/jocn.2008.21029
45. Kuzmanovic B, Bente G, von Cramon DY, Schilbach L, Tittgemeyer M, Vogele K. Imaging first impressions: Distinct neural processing of verbal and nonverbal social information. *NeuroImage.* (2012) 60:179–88. doi: 10.1016/j.neuroimage.2011.12.046
46. Spunt RP, Adolphs R. The neuroscience of understanding the emotions of others. *Neurosci Lett.* (2019) 693:44–8. doi: 10.1016/j.neulet.2017.06.018
47. Dean DC 3rd, Freeman A, Lainhart J. The development of the social brain in baby siblings of children with autism. *Curr Opin Psychiatry.* (2020) 33:110–6. doi: 10.1097/YCO.0000000000000572
48. Padmanabhan A, Lynch CJ, Schaefer M, Menon V. The default mode network in autism. *Biol Psychiatry Cognit Neurosci Neuroimag.* (2017) 2:476–86. doi: 10.1016/j.bpsc.2017.04.004
49. Ben-Sasson A, Hen L, Fluss R, Cermak SA, Engel-Yeger B, Gal E. A meta-analysis of sensory modulation symptoms in individuals with autism spectrum disorders. *J Autism Dev Disord.* (2009) 39:1–11. doi: 10.1007/s10803-008-0593-3
50. Marco EJ, Hinkley LBN, Hill SS, Nagarajan SS. Sensory processing in autism: a review of neurophysiologic findings. *Pediatr Res.* (2011) 69:48–54. doi: 10.1203/PDR.0b013e3182130c54
51. Mottron L, Dawson M, Soulières I, Hubert B, Burack J. Enhanced perceptual functioning in autism: an update, and eight principles of autistic perception. *J Autism Dev Disord.* (2006) 36:27–43. doi: 10.1007/s10803-005-0040-7
52. Edwards LA. A meta-analysis of imitation abilities in individuals with autism spectrum disorders. *Autism Res.* (2014) 7:363–80. doi: 10.1002/aur.1379
53. Williams JHG, Whiten A, Singh T. A systematic review of action imitation in autistic spectrum disorder. *J Autism Dev Disord.* (2004) 34:285–99. doi: 10.1023/B:JADD.0000029551.56735.3a
54. Vincent JL, Kahn I, Snyder AZ, Raichle ME, Buckner RL. Evidence for a frontoparietal control system revealed by intrinsic functional connectivity [published correction appears in *J Neurophysiol.* 2011 Mar;105(3):1427]. *J Neurophysiol.* (2008) 100:3328–42. doi: 10.1152/jn.90355.2008
55. Ocasio W. Attention to attention. *Organ Sci.* (2011) 22:1286–96. doi: 10.1287/orsc.1100.0602